Extrinsic and Intrinsic Index Finger Muscle Attachments in an OpenSim Upper-Extremity Model

Jong Hwa Lee, Deanna S. Asakawa, Jack T. Dennerlein & Devin L. Jindrich

Annals of Biomedical Engineering
The Journal of the Biomedical Engineering Society

ISSN 0090-6964

Ann Biomed Eng
DOI 10.1007/s10439-014-1141-2

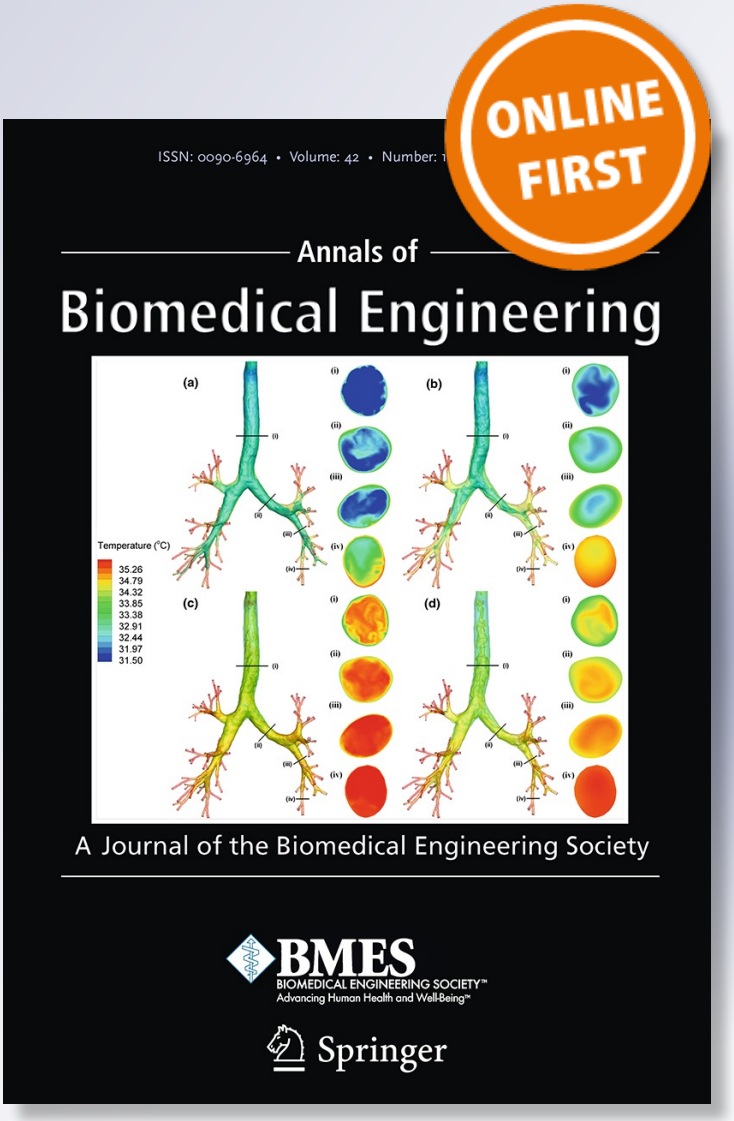

Springer

Annals of Biomedical Engineering (© 2014)
DOI: 10.1007/s10439-014-1141-2

BMES BIOMEDICAL ENGINEERING SOCIETY™ www.bmes.org

Extrinsic and Intrinsic Index Finger Muscle Attachments in an OpenSim Upper-Extremity Model

JONG HWA LEE,[1] DEANNA S. ASAKAWA,[2] JACK T. DENNERLEIN,[3] and DEVIN L. JINDRICH[2]

[1]Department of Mechanical and Aerospace Engineering, Arizona State University, Tempe, AZ, USA; [2]Department of Kinesiology, California State University San Marcos, 333 S. Twin Oaks Valley Rd., University Hall 302, San Marcos, CA 92096, USA; and [3]Department of Physical Therapy, Movement, and Rehabilitation Sciences, Bouvé College of Health Sciences, Northeastern University, Boston, MA, USA

(*Received 8 June 2014; accepted 23 September 2014*)

Associate Editor Peter E. McHugh oversaw the review of this article.

Abstract—Musculoskeletal models allow estimation of muscle function during complex tasks. We used objective methods to determine possible attachment locations for index finger muscles in an OpenSim upper-extremity model. Data-driven optimization algorithms, Simulated Annealing and Hook-Jeeves, estimated tendon locations crossing the metacarpophalangeal (MCP), proximal interphalangeal (PIP) and distal interphalangeal (DIP) joints by minimizing the difference between model-estimated and experimentally-measured moment arms. Sensitivity analysis revealed that multiple sets of muscle attachments with similar optimized moment arms are possible, requiring additional assumptions or data to select a single set of values. The most smooth muscle paths were assumed to be biologically reasonable. Estimated tendon attachments resulted in variance accounted for (VAF) between calculated moment arms and measured values of 78% for flex/extension and 81% for ab/adduction at the MCP joint. VAF averaged 67% at the PIP joint and 54% at the DIP joint. VAF values at PIP and DIP joints partially reflected the constant moment arms reported for muscles about these joints. However, all moment arm values found through optimization were non-linear and non-constant. Relationships between moment arms and joint angles were best described with quadratic equations for tendons at the PIP and DIP joints.

Keywords—Hand, Finger, Arm, Moment arm, Muscle geometry, Musculoskeletal, Optimization, Simulated annealing, Variability, Redundancy.

Address correspondence to Devin L. Jindrich, Department of Kinesiology, California State University San Marcos, 333 S. Twin Oaks Valley Rd., University Hall 302, San Marcos, CA 92096, USA. Electronic mail: djindrich@csusm.edu

INTRODUCTION

Multitouch human computer interfaces (HCIs), such as the touchscreens of many handheld devices, often involve complex multi-finger gestures or gesture sequences.[56,58,67] Although the forces involved in making individual gestures may be low, long-term and repetitive interactions with touchscreen computing devices present the potential for injury.[8] However, the biomechanics of coordinated finger movements for touchscreen interaction are not well understood. Consequently, better understanding of finger dynamics, joint forces, and control during multitouch tasks could lead to interface designs that reduce injury risks associated with repetitive finger movements.

External hand and finger loadings do not directly correspond to internal musculoskeletal loading, which can be difficult to determine.[54] However, anatomically based musculoskeletal models can predict musculoskeletal loading and can help design strategies to reduce injury and improve motor function.[16,20,39,44,61] Anatomical studies of the elbow and shoulder enabled development of detailed arm musculoskeletal models.[17,23,51] Arm models can estimate torques at the shoulder and elbow, e.g., for development and user training of neural prosthesis systems.[13,22,29,62] Hand models have also been useful for understanding many aspects of function such as finger tapping on computer keyboards.[3,5,37,52,53,57,59,69] Although hand models have been helpful in specific contexts, existing dynamic models of the hand often focus on specific fingers and have not been used to understand complex, multi-finger gestures such as those used during multitouch HCI tasks.

We therefore seek to develop a musculoskeletal model capable of estimating internal loadings during

Published online: 04 October 2014

multitouch tasks. Because multitouch and gestural movements involve not only the fingers, but also the entire kinematic chain of the hand and arm, we chose to build upon an existing arm model available on an open access platform (OpenSim 2.3.2, Simbios, Stanford, CA.[15]). The model incorporates information for muscles at the shoulder and elbow, but it does not yet model intrinsic finger muscles. OpenSim is a homeomorphic model: parameters and values correspond directly to anatomical structure and function. Therefore, appropriate muscle attachment sites within the anatomy of the OpenSim model must be determined. Detailed measurements of muscle attachments have been made for the hand.[3,36] However, muscle attachment locations are specific to the anatomical model within which they are expressed, and cannot be directly transformed to a different model such as OpenSim. For example, the model of An *et al.*[3] is normalized only to the middle phalanx in a 2 dimensional (2D) sagittal plane, and scaling its attachment locations in a 3D Cartesian space (c.f. Refs. 24,38) does not result in continuous moment arms that match experimentally measured values.[34] This poor correspondence could result from a lack of important information such as joint thickness, position and orientation of rotational axes, skeletal structure, and changes associated with transforming from 2 to 3 dimensions among other factors.

To create the most functionally useful model possible, we chose to use moment arm data for the index finger measured *in vivo*[40,50,68] and *in situ*.[4,5,10,14,19] However, measurements of moment arms alone cannot be directly used to develop homeomorphic models because moment arms are indeterminate: many combinations of origins and insertions, or paths, could result in the same moment arm. The purpose of this study was therefore to determine a set of muscle attachment points for the tendons and intrinsic muscles of the index finger. We focused on the question: can data-driven optimization find reasonable attachment sites for extrinsic tendons and intrinsic muscles? We hypothesized that Simulated Annealing[33] could find muscle attachment points for extrinsic and intrinsic finger tendons and muscles, resulting in moment arms that match experimentally-measured curves over the entire joint range of motion.

MATERIALS AND METHODS

We used the Holzbaur *et al.*[29] upper extremity model on the OpenSim platform (2.3.2, Simbios, Stanford, CA.[15]). Currently, the shoulder, elbow, forearm, wrist, thumb, and index finger are modeled with 15 joint degrees of freedom and 50 muscle compartments. Metacarpal and phalanx geometry, and approximated positions and orientations of finger joint axes, are scaled to a 50th percentile male. Axes of rotation were determined by fitting long axes of cylinders to the articular surfaces of the metacarpal and phalangeal bones.[29]

Musculoskeletal Model

We added the following muscles or muscle groups to the index finger of OpenSim model: *terminal extensor (TE), extensor slip (ES), radial band (RB), ulnar band (UB), first dorsal interosseous or radial interosseous (RI), lumbricals (LU), first palmar interosseous or ulnar interosseous (UI), flexor digitorum profundus (FDP), flexor digitorum superficialis (FDS) and extensor digitorum communis (EDC)*. The index finger was modeled to have four degrees of freedom (DOFs). The metacarpophalangeal (MCP) joint has 2 DOFs: ab/adduction and flex/extension. Both the proximal interphalangeal (PIP) and distal interphalangeal (DIP) joints are modeled to have one DOF: flex/extension. Based on experimental measurements available for comparison, we limited our analysis to the following range of motion (RoM) at the MCP joint: 0°–90° (flexion: +) as well as 0°–30° (abduction: +). Similarly, for PIP and DIP joints we considered 0°–90° (flexion: +) and 50° (flexion: +) respectively.[4,14] The model included the Holzbaur *et al.*[29] wrap objects for the extrinsic tendons, and we created new wrap objects for the intrinsic muscles that conformed to the bone shape.

Moment Arms

Experimentally measured values were used as reference moment arms.[3–5,14] More recent studies have measured moment arms for one muscle (FDS) using more sophisticated techniques.[42] However, we chose to base our model on datasets reporting both extrinsic and intrinsic muscles to maintain consistency of source specimens and measurement techniques among muscles. For the MCP joint, we extracted 10 data points (x: joint angles, y: moment arm values) from published moment arm curves[4,14] using the GRABIT function (Matlab 2010b, Mathworks, Natick, MA). We recreated moment arm curves (vs. angle of rotation) for the optimization using a Polynomial Curve Fitting function (*polyfit*; 5th degree polynomial) in Matlab. For PIP and DIP joints, moment arm curves have not been reported. Therefore, constant moment arms (averaged through the RoM of 0°–90° and 50°) were used.[4]

To normalize for differences among data sets and reproduce finger skin surface from the bony segments in the OpenSim model, we assumed all linear dimensions

scaled isometrically, as found for the ratio among the length of phalanx, the width and thickness of each joint.[18,24,38] We scaled measured anthropometric data to the OpenSim model dimensions to describe muscle–tendon paths within OpenSim (Table 1), then normalized moment arms to the length of the middle phalanx.[3]

Muscle Attachment Determination

A data-driven optimization method was used to identify muscle paths determining model-optimized moment arms to be matched with experimentally-measured values over the joint RoM. The optimization consists of three parts: (1) objective function, (2) boundary conditions and (3) inequality constraint. First, the objective function, $f(\vec{x})$ was defined as the root mean square (RMS) error between the experimentally derived moment arms, $r_j(\vec{q}_i)$ and the model-estimated moment arms, $\hat{r}_j(\vec{q}_i, \vec{x})$ as follows:

$$\text{Minimize } f(\vec{x}) = \sqrt{\sum_{i=1}^{m} \frac{\left[r_j(\vec{q}_i) - \hat{r}_j(\vec{q}_i, \vec{x})\right]^2}{m}}$$

$$\text{Subject to } lb_j \leq x_j \leq ub_j$$

$$g_j(\vec{x}) - \varepsilon_j \leq 0$$

where j was each individual muscle ($j = 10$), and $\vec{x}$ was 6×1 vector (described as x, y, z origin points on the proximal side and x, y, z insertion points on the distal side) to be optimized. $\vec{q}_i$ was the joint angle with a resolution (i) of 100 increments (m) covering the RoM of measured values[4]: the 0°–90° (flexion) and 0°–30° (abduction), 0°–90° (flexion), and 0°–50° (flexion) for the MCP, PIP and DIP joints, respectively. Moment arm curves vary in magnitude and shape at every joint. However, lacking criteria to differentially weight different joints, we summed RMS errors for each muscle over all joints in the objective function.

Second, boundary conditions ($lb_j \leq x_j \leq ub_j$) constrained the path of a muscle from violating a feasible region extending from the bone (a lower bound: lb_j,[29] to the finger skin surface (an upper bound: ub_j,[18,24,38]).

Third, an inequality constraint was imposed on both flex/extension and ab/adduction. Attachment points must result in moment arms appropriate for both flex/extension and ab/adduction. However, measurements for flex/extension and ab/adduction did not have equal reliability, reflected in different reported standard deviations that could reflect either measurement uncertainty or anatomical variability[3–5,14]; Moreover, ab/adduction moment arm values depend on finger postures, i.e., flexion of MCP, PIP and DIP joints.[30] The specific postures used for measured ab/adduction moment arm values were not reported, contributing to uncertainty. Therefore, we did not consider both flex/extension and ab/adduction moment arm values as a same weight in the objective function. However, we did not have an objective criterion for assigning specific differential weightings between flex/extension and ab/adduction. Instead, we used an inequality constraint. The objective function minimized flex/extension RMS errors ($f(\vec{x})$) subject to the inequality constraint, which required valid muscle attachments ($\vec{x}$) to result in moment arms within experimentally measured standard deviations ($g_j(\vec{x}) \leq \varepsilon_j$). The inequality constraint resulted in punishment if the RMS error of ab/adduction moment arm during flex/extension ($g_j(\vec{x})$) exceeded the bounds of the maximum standard deviation of experimental moment arms ε_j. Specifically, min. $f(\vec{x})$ = RMS error + $P(\vec{x})$. $P(\vec{x})$, the penalty function, is zero if $g_j(\vec{x}) \leq \varepsilon_j$. $P(\vec{x}) = \varepsilon_j \emptyset$ if $g_j(\vec{x}) > \varepsilon_j$, where $\emptyset = 1000$. ε_j was 2.5 mm for extrinsic tendons and 1.7 mm for intrinsic muscles. Therefore, because extrinsic muscle ab/adduction moment arms had higher uncertainty than those of intrinsic muscles, attachment points were less influenced by the ab/adduction moment arms for extrinsic muscles than for intrinsic muscles.

TABLE 1. Anthropometric finger dimensions of cadaveric specimens An (1983) and OpenSim model (mm).

	Specimens bony dimensions	OpenSim bony dimensions	Skin surface scaled
Distal phalanx length	19.67 ± 1.03	19.10 (Δ0.57)	30.65
Middle phalanx length	24.67 ± 1.37	25.10 (Δ0.43)	27.22
Proximal phalanx length	43.57 ± 0.98	42.60 (Δ0.97)	50.86
DIP joint thickness	5.58 ± 0.92	4.95 (Δ0.63)	14.38
PIP joint thickness	7.57 ± 0.45	7.31 (Δ0.26)	18.86
MCP joint thickness	15.57 ± 0.84	17.08 (Δ1.51)	27.80

Symbol (±) indicates standard deviation in interspecimen variation. Lengths of the phalanges in the OpenSim model are calculated as the distance between the origins of two coordinate systems in 3D Cartesian space, e.g., the center of rotation at MCP and the center of rotation at PIP. Parentheses (Δ) in OpenSim bony dimensions express difference between model dimensions and specimen dimensions. The skin surface set was scaled in 3D to preserve the anatomical proportions of Fowler *et al.*,[18] Greiner[24] and Li *et al.*[38] The skin surface (external dimensions) functioned as an upper boundary constraint during optimization.

PIP and DIP joints are modeled to move only in flex/extension. Therefore, the inequality constraint for PIP and DIP joints favored attachments that optimized moment arms while maintaining tendon excursions within measured variance. ε_j was therefore set to the measured standard deviation (0.72–3.97 mm) of tendon excursions.[4,5,14]

The objective function for each individual muscle (j) was computed for each set of parameters, then iterated by updating muscle attachment locations until an optimal set was found. We used Simulated Annealing[33] and Hooke-Jeeves[31] algorithms. The Simulated Annealing algorithm used a cooling schedule with initial temperature of 1, and iterated until the average change in value of the objective function was less than 0.0001. The maximum number of evaluations of the objective function was 18,000 (3000 × 6 variables).

Sensitivity Analysis

Optimizations in complex search spaces can be influenced by initial parameter selection.[2,63] Therefore, to test the robustness of the finger model response ($\vec{x}_j$) to input ($\vec{x}_0$), we performed sensitivity analysis for all attachments ($\vec{x}_j$) by randomly selecting 26 starting points ($\vec{x}_0$), including the Holzbaur *et al.*[29] OpenSim model attachments and estimates of the An *et al.*[3] tendon locations. Because the middle phalanx is ~25 mm,[4] 26 increments can cover the length of the middle phalanx at 1 mm resolution. Consequently, 78,000 simulations (26 trials × 3000 objective function evolutions) were performed for each muscle at each joint.

The sensitivity analyses showed that minimizing RMS error alone resulted in multiple possible muscle paths, some of which involved sharp changes to tendon direction (Fig. 1). The potential for multiple muscle attachments and paths necessitated the selection of a single set of attachment points. We therefore assumed that the most smooth muscle path was the most anatomically reasonable. We calculated curvature from three successive attachments, i.e., origin, via and insertion points and identified the attachment set with the largest curvature at each joint. We selected the path with the largest curvature for analysis and presentation.

Consequently, our procedure accomplished two objectives. The most important objective was to discover muscle attachment points that resulted in moment arms that matched experimentally measured values in both flex/extension and ab/adduction. From the set of optimized attachment points, a single set of points was selected to satisfy the secondary objective of path smoothness. This two-step procedure ensured that the primary, functional objective of discovering the most experimentally reasonable moment arms was not overly influenced by the assumption that smooth muscle paths were the most anatomically reasonable.

To test the hypothesis that optimization could successfully find moment arm curves, we determined whether the RMS error between optimized and experimentally measured moment arms were within measured variability (one experimentally measured standard deviation (SD)).

Polynomial Fitting

We determined the order and parameters of polynomial fits that could be used as simplified descriptions of moment arm curves. We used a fitting function to determine the coefficients of a polynomial of degree n that fit the simulated moment arms. We tested polynomials of less than fourth degree because polynomials of greater order can overfit to the data and even perform worse than lower-order regressions.[35,46] To measure the agreement between model-optimized and experimentally measured moment arm curves, we used the variance accounted for (VAF), computed as

$$\mathrm{VAF} = 100 \times \left(1 - \sqrt{\sum \left(\vec{r} - \hat{\vec{r}}\right)^2} / \sqrt{\sum \vec{r}^{\,2}}\right)$$

Optimizations and data analysis were implemented in Matlab, using the OpenSim Application Programming Interface (API; OpenSim 2.0 Doxygen) to compute muscle moment arms.

RESULTS

Optimization Found Multiple Sets of Muscle Attachments

The optimization procedure found multiple muscle attachments (Fig. 2). For some muscles, attachment points were constrained to a narrow region. For example, the standard deviation for FDS at the MCP joint was 0.6 mm. For other muscles, attachment points could be located in a broad region. For example, the ES at the PIP joint had a standard deviation of 1.7 mm. Still other muscles exhibited distinct alternative attachment regions. For example, RI at the MCP joint showed two alternative attachment regions, resulting in a bimodal distribution and large standard deviation of 9.0 mm. Although multiple sets of muscle attachments were possible, the different muscle attachments resulted in consistent moment arm curves. Compared to each other, the average VAF among optimized curves was of 94% across all attachment sets and muscles.

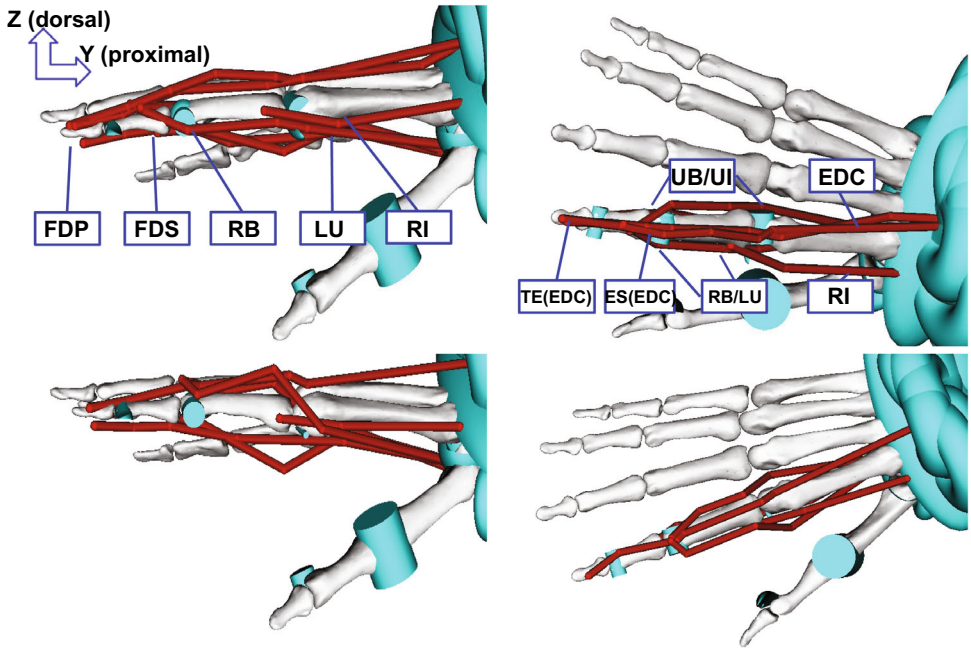

FIGURE 1. Musculoskeletal hand model. Sagittal and transverse view. Upper two pictures represent smoothest muscle paths, and lower two pictures represent minimum RMS error muscle paths. The *x*-axis (flexion–extension) is projected radially for the left hand and ulnarly for the right hand: flex(+)/extension(−), the *y*-axis is projected along the phalangeal or the metacarpal shaft passing from the distal to proximal side: ulnar twist(+)/radial twist(−), and the *z*-axis (radioulnar) is projected dorsally: ab(+)/adduction(−). The coordinate system in the OpenSim model is right-handed using homogeneous transforms.

Optimized Moment Arms Matched Experimentally Measured Values

The smoothest muscle paths chosen to represent the most anatomically reasonable set of muscle attachments had moment arms that matched experimental measurements and were representative of the set of optimized moment arms (Tables 2 and 3; Figs. 3a and 3b). At the MCP joint, all modeled moment arms, including those from the smoothest path, lay within one standard deviation of experimental measurements (max. RMS error = 2.4 mm < max. experimental SD = 2.5 mm[4]). For both flex/extension and ab/adduction motions, VAF between experimentally measured values and smoothest-path modeled moment arms averaged 78% (flex/extension) and 81% (ab/adduction), and ranged from 48 to 99%. For most muscles, the smoothest-path moment arms were within one standard deviation of the average calculated moment arms. For the EDC muscle in flex/extension, the smoothest-path moment arm differed from the average (VAF = 48%) but was closer to the experimentally measured moment arm (RMS error = 0.7 mm < experiment SD = 1.6 mm).

At the PIP and DIP joints, only average moment arms have been reported. VAF between calculated and reported moment arms averaged 67 and 54% for PIP and DIP joints. Modeled moment arms from the smoothest path were located within one standard deviation of measured values (average RMS error = 1.9 ± 1.5 mm < max. experimental SD = 2.5 mm; Fig. 3).

Calculated Moment Arms at the PIP and DIP Joints were Not Constant

Experimental moment arms for the PIP and DIP joints were considered to be near constants.[4] For example, at the PIP joint, experimentally measured moment arms of extrinsic tendons were reported as: $r_{fdp} = 7.9$, $r_{fds} = 6.2$ and $r_{es} = -2.8$ mm.[4] However, optimization did not discover constant moment arms for any muscle at the PIP and DIP joints.

Calculated moment arms were non-constant and non-linear functions of joint angle ($0 \le q \le 2.09$ rad.; Fig. 3). VAF of calculated moment arms with respect to constants averaged 83% whereas fitting calculated moment arms with linear functions resulted in average VAF of 93%, quadratic of 99% and cubic of 100%. Because quadratic fits were substantially (5.5%) better than linear fits, but had only 1.3% less VAF than cubic fits, we considered quadratic functions to be the lowest-degree functions that adequately fit the moment arms. Quadratic functions for the PIP were: $r_{fdp} = -3.01q^2 + 5.82q + 5.84$, $r_{fds} = -3.26q^2 + 5.29q + 4.75$ and $r_{es} = 0.56q^2 + 3.85q - 6.82$. Similar reasoning led to fitted curves for intrinsic muscles around the PIP joint of $r_{ub} = -0.74q^2 + 1.94q + 0.69$,

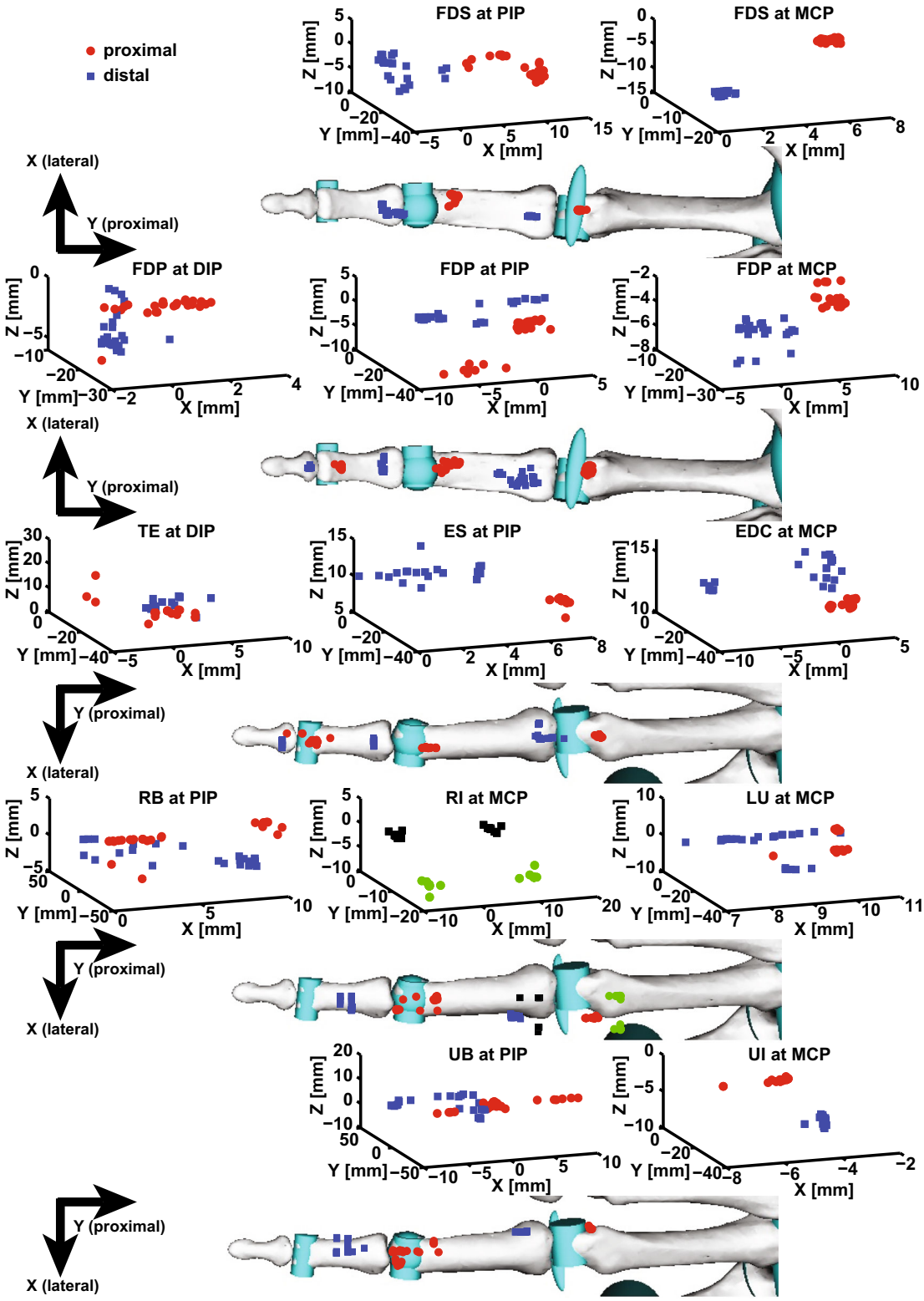

FIGURE 2. Muscle attachment points for modeled muscles at the MCP, PIP and DIP joints. Red circles (green for RI) indicate proximal points, and blue squares (black for RI) indicate distal points.

TABLE 2. Moment arms (MA) of muscle paths discovered through optimization (mm).

Joint	RoM	FDP	FDS	EDC(ES)	LU(RB)	RI	UI(UB)	
MCP	Flex/Ext	0°–90°	11.6 ± 0.5	12.3 ± 0.9	−6.7 ± 0.6	3.0 ± 0.6	5.9 ± 0.6	3.6 ± 1.1
			11.5(Δ0.2)	12.4(Δ0.1)	−7.4(Δ0.7)	3.8(Δ1.0)	5.4(Δ2.5)	3.3(Δ1.8)
	Ab/Add	0°–30°	2.9 ± 0.6	1.7 ± 0.6	−1.8 ± 0.5	5.7 ± 0.7	5.5 ± 0.9	−6. ± 0.8
			2.8(Δ0.8)	1.5(Δ0.5)	−1.0(Δ0.1)	6.5(Δ2.2)	5.6(Δ1.3)	−6.9(Δ0.5)
PIP	Flex/Ext	0°–90°	7.5 ± 0.7	6.4 ± 0.2	−3.6 ± 0.1	1.9 ± 0.3		0.1 ± 0.4
			7.1(Δ1.3)	6.2(Δ0.7)	−3.3(Δ2.2)	1.9(Δ3.8)		1.6(Δ4.2)
DIP	Flex/Ext	0°–50°	3.4 ± 0.7		−3.3 ± 1.9			
			4.1(Δ0.5)		−0.9(Δ0.8)			

Values conform to OpenSim conventions: flex(+)/extension(−) and ab(+)/adduction(−) at DIP, PIP and MCP joints. Mean MA of multiple muscle paths (top values) are represented with standard deviations (±). Mean MA of single muscle paths (bottom values) are represented with RMS error (Δ) between smoothest path and experimental values.[4]

$r_{rb} = -0.92q^2 + 2.05q + 1.05$, and muscles about the DIP joint of $r_{fdp} = -1.12q^2 + 3.07q + 3.09$ and $r_{te} = 0.29q^2 + 1.36q - 1.56$.

DISCUSSION

The primary goal of this study was to use data-driven optimization to determine muscle–tendon paths for a musculoskeletal model of the index finger. Simulated Annealing and Hooke-Jeeves algorithms successfully found muscle–tendon pathways, resulting in moment arms that matched experimentally measured curves. Optimization also suggested that moment arms at the PIP and DIP joints are primarily non-linear and non-constant over the range of motion.

Limitations

Several limitations of our approach should be considered when evaluating these conclusions. First, we used simple wrapping surfaces that in some circumstances can result in discontinuous moment arm curves.[29] To our knowledge, quantitative measurements that could be used to create more anatomically based wrapping surfaces are not generally available for finger muscles. Optimization could be used to determine wrapping object parameters that result in moment arms that match experimental data.[22] Although these wrapping surfaces could potentially improve muscle paths, validating the wrapping surfaces or resulting muscle paths would not have been possible with existing data. Therefore, we chose to use the parsimonious approach possible.

Second, we modeled muscle attachment sites as single points. Muscles attach to bones and tendons with contact areas of varying size. However, point contacts can be considered equivalent systems that replace distributed loads with a simplified representation,[25] and have been successfully used in several contexts.[21,45]

Third, hand specimens used for experimental measurements are variable in size, and none precisely match the hypothetical 50th percentile male of the OpenSim model. We tried to minimize potential errors by normalizing not only by middle phalanx length, but also by MCP thickness for flex/extension moment arms and MCP width for ab/adduction values. Consequently, our model's anthropometric dimensions lie within one standard deviation of the mean for experimental specimens (Ref. 4; Table 1).

Fourth, we were not able to directly compare the muscle attachment points found through optimization to anatomical measurements. Direct transformation between the 2D coordinate system used by An *et al.*[3] and the 3D Opensim model is difficult because of several unknowns, including differences in bone segment ratios, the relative locations of coordinate system origins, and differences in 3D segment orientations. However, there are several reasons that we consider the anatomical locations of the attachment points reasonable. First, qualitative comparisons to finger anatomy (Fig. 2) suggest that the muscle attachments are reasonable. Second, moment arms calculated using the partial velocity method from the muscle attachments of An *et al.*[3] match the measured moment arms of An *et al.*[4] used for optimization (Lee *et al.*, in prep). Given that optimization did not find extremely divergent attachment locations (Fig. 2), the agreement of moment arms calculated from measured and optimized attachments suggests that each set of attachments is reasonable within their own frame of reference.

Finally, we did not perform experimental studies to validate the model at a functional level.[63] Full model validation would require determination of muscle physiological parameters, estimation of muscle activation, and comparison to experimentally measured output during several different tasks, and was therefore outside the scope of the present study. However,

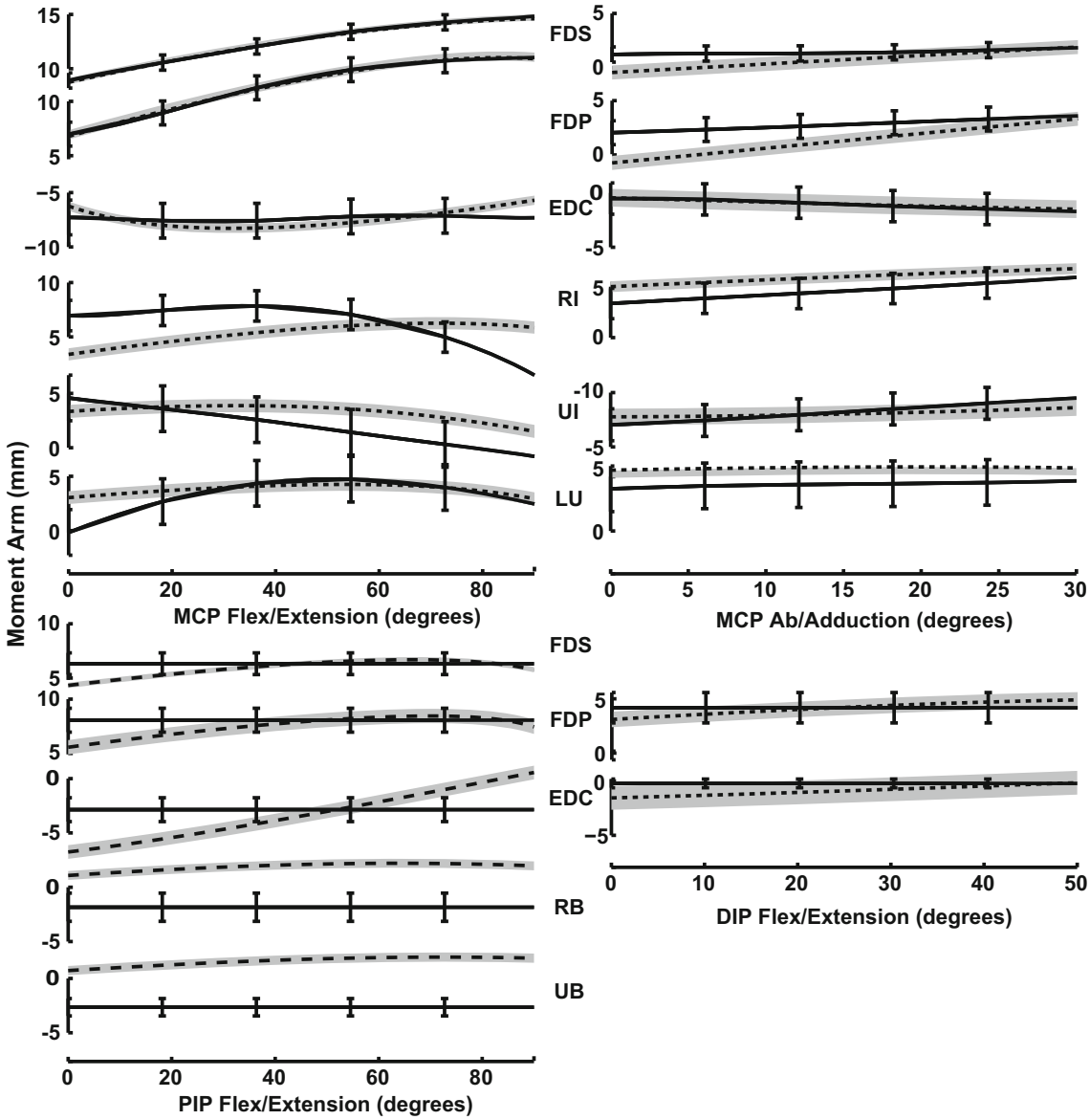

FIGURE 3. Moment arms for smoothest muscle paths compared to experimental values. Solid lines represent average experimentally measured (n = 7) moment arms, with standard deviations indicated by error bars.[4] Dotted lines represent modeled moment arms of the smoothest muscle paths. Gray bands represent one standard deviation above and below average modeled moment arms from all calculated sets of muscle attachments. Average calculated moment arms are in the center of the gray bands, but are not shown for clarity.

at the anatomical level, we demonstrated that optimization could determine muscle attachments that resulted in moment arm curves that matched experimental measurements. Future modeling and experimental work will be necessary to resolve discrepancies among experimental measurements,[4,5,42] and fully validate the model.

Moment Arms are Reasonable Approximations of Experimentally Measured Values

Modeled moment arms fitted experimentally measured values, lying within one experimental standard deviation for joints where variances were available. These findings therefore support our hypothesis that data-driven optimization can be used to determine moment arms for musculoskeletal models.

Optimization is Useful for Data-Driven Model Development

Our results are consistent with a growing number of studies showing that optimization can contribute to musculoskeletal model development. Simulated annealing (SA) algorithms can outperform gradient and simplex methods.[47,64] SA therefore represents a

TABLE 3. Muscle-tendon locations (mm) of the index finger, expressed in OpenSim frame.

Joint	Muscles	*x*	*y*	*z*	*x*	*y*	*z*
		Proximal point (secondmc)			Distal point (proxph2)		
MCP	FDP	4.11 (9.11)	−16.00 (−15.99)	−4.21 (−4.21)	3.34 (−0.34)	−20.24 (−19.70)	−5.03 (−5.03)
	FDS	4.86 (5.86)	−13.77 (−13.77)	−0.66 (−0.66)	1.32 (2.09)	−8.41 (−8.41)	−12.01 (−12.01)
	RI	9.07 (−8.03)	−19.95 (−16.51)	−4.88 (−12.32)	7.04 (0.13)	−6.72 (−9.03)	−0.15 (−4.36)
	LU	10.17 (10.19)	−26.47 (−27.82)	−0.01 (−0.34)	8.38 (10.24)	−8.29 (−9.75)	0.04 (9.87)
	UI	−3.32 (−5.10)	−29.39 (−30.00)	−0.12 (−0.25)	−4.31 (−3.00)	−15.93 (−16.57)	2.41 (−8.13)
	EDC	3.05 (3.05)	−29.51 (−29.51)	12.43 (12.43)	3.31 (3.31)	−7.11 (−7.11)	11.64 (11.64)
		Proximal point (proxph2)			Distal point (midph2)		
PIP	FDP	2.74 (1.51)	−36.50 (−36.50)	1.27 (1.27)	−1.84 (−3.07)	−9.84 (−9.84)	−2.70 (−2.70)
	LU (RB)	13.15 (14.99)	−39.58 (−39.92)	3.77 (8.36)	2.21 (1.35)	−17.25 (−2.20)	5.84 (5.65)
	UI (UB)	0.18 (−0.14)	−39.99 (−31.69)	7.79 (9.95)	3.83 (2.78)	−13.75 (−2.03)	4.87 (5.88)
	FDS	6.35 (3.35)	−36.78 (−36.78)	2.32 (2.32)	1.31 (1.31)	−19.04 (−19.04)	−3.40 (−3.39)
	EDC (ES)	5.15 (6.88)	−27.71 (−38.72)	11.15 (9.95)	2.17 (1.86)	−2.69 (−0.10)	7.65 (5.41)
		Proximal point (midph2)			Distal point (distph2)		
DIP	FDP	1.32 (0.17)	−20.96 (−24.35)	−1.65 (3.05)	1.56 (1.56)	−10.19 (−10.19)	−2.92 (−2.92)
	EDC (TE)	0.40 (0.17)	−23.54 (−24.35)	3.29 (3.05)	0.49 (2.63)	−10.67 (−8.07)	2.29 (1.63)

The coordinate system of the OpenSim model is attached to metacarpal (secondmc), proximal (proxph2), middle (midph2) and distal (distph2) phalanges, respectively. *x*, *y* and *z* components indicate radioulnar (+ points out, perpendicular to the palm plane), axial (+ points from distal to proximal side), and dorsolar (+ points up, from palm to hand side) respectively. *x*, *y* and *z* values represent smoothest muscle paths, and parentheses () values of *x*, *y* and *z* represent minimum root mean square (RMS) difference muscle paths.

technique that can help provide data-driven solutions for diverse applications.[26,27,41,43,48,49,60,71] Using optimization reduces subjective judgments, and could be useful for rapid and reliable model customization.

Multiple Attachments Produced the Same Moment Arm Values

Optimization found multiple attachment points ($\vec{x}_j$) that resulted in similar moment arms. These multiple attachment sets are analogous to anatomical variability among individuals commonly observed in hand and finger muscle attachments. For example, lumbrical (LU) muscles show deviations in the origins and insertions.[7,65] Single tendons of extensor pollicis longus (EPL) were observed in 67.4% of hands, whereas duplicated tendons were detected in 8.3–32.6%.[1,12] Moment arm determines the change in musculotendon length and musculotendon velocity during joint movement[4,16] and muscle contributions to joint stiffness[28]. Therefore, although function (i.e., moment arms) may be constrained, several anatomical configurations may be available to achieve equivalent function. Optimization based on functional objectives could therefore represent another strategy for the important goal of being able to adapt musculoskeletal models to individual differences, and suggest potential alternative attachment sites.[6]

Modeled Moment Arms are Non-linear and Non-constant

Experimentally measured moment arms were reported to be nearly-constant values in flex/extension for muscles at PIP and DIP joints.[4,14] Constant moment arms occur when the line connecting distal insertion points and proximal origin points is parallel to joint segments in a fully-extended posture. Moment arms calculated using Landsmeer's model are constants. The approximation of constant moment arms could have resulted from the projection of muscle attachment locations in Cartesian space (3D) onto the sagittal plane (2D) during experimental measurements. However, muscle attachment points are not anatomically parallel to phalanx bones.[3,4,70] Consequently, moment arms have been reported to vary as a function of joint angle at the PIP and DIP joints in simulation,[66] *in vitro*,[19] and *in vivo*[18] studies. The moment arms found by optimization were also non-constants that depended on joint angle at PIP and DIP joints. Moreover, moment arms at other hand joints are also non-linear curves.[4,9,11,19,32,34] Our findings that quadratic functions provide reasonable expressions for moment arms are consistent with studies of flexor tendons of the hand, which can be expressed with quadratic fits.[19] Although we found quadratic fits to be sufficient to represent the moment arms of index

fingers, more sophisticated strategies may be necessary to describe musculotendon lengths and moment arms for time-limited computational models.[55]

In conclusion, using optimization resulted in three primary discoveries. First, moment arm values calculated from optimization solutions can match experimental values, demonstrating that data-driven optimization approaches can be used to generate musculoskeletal models while reducing subjective judgments or estimations. Second, multiple sets of muscles attachments with similar optimized moment arms are possible, presenting the question of whether some of the anatomical variability observed does not substantially affect motor function. Third, moment arms for muscles around the PIP and DIP joints are not constant, but can be modeled with quadratic functions consistent with other muscles. Including anatomical data for finger musculature into the OpenSim arm model will result in a more complete musculoskeletal model that can be useful in many areas, including quantitative analysis of internal loading during multitouch and HCI tasks.

ACKNOWLEDGMENTS

This work was supported by a Grant from the National Science Foundation (NSF 0964220). We thank Cecil Lozano for initial contributions to the project. We thank Aaron Kociolek and Alexander MacIntosh (McMaster University) and Christopher Gatti, (Rensselaer Polytechnic Institute) for sharing their OpenSim models. We wish to express our deep gratitude to Dr. Kai-Nan An (Mayo Clinic College of Medicine) and Dr. John Z. Wu (National Institute for Occupational Safety) for helpful discussions regarding coordinate transformation. Moreover, we would like to thank Dr. Panagiotis Artemiadis, Patrick Phelan, Veronica Santos and Huei-Ping Huang for their valuable comments on this study.

REFERENCES

[1]Abdel-Hamid, G. A., R. A. El-Beshbishy, and I. H. Abdel Aal. Anatomical variations of the hand extensors. *Folia Morphol.* 72(3):249–257, 2013.

[2]Ackland, D. C., Y. C. Lin, and M. G. Pandy. Sensitivity of model predictions of muscle function to changes in moment arms and muscle-tendon properties: a Monte Carlo analysis. *J. Biomech.* 45:1461–1471, 2012.

[3]An, K. N., E. Y. Chao, W. P. Cooney, and R. L. Linscheid. Normative model of human hand for biomechanical analysis. *J. Biomech.* 12:775–788, 1979.

[4]An, K. N., Y. Ueba, E. Y. Chao, W. P. Cooney, and R. L. Linscheid. Tendon excursion and moment arm of index finger muscles. *J. Biomech.* 16:419–425, 1983.

[5]Armstrong, T. J., and D. B. Chaffin. An investigation of the relationship between displacements of the finger and wrist joints and the extrinsic finger flexor tensions. *J. Biomech.* 11:119–128, 1978.

[6]Arnold, A. S., S. Salinas, D. J. Asakawa, and S. L. Delp. Accuracy of muscle moment arms estimated from MRI-based musculoskeletal models of the lower extremity. *Comput. Aided Surg.* 5:108–119, 2000.

[7]Basu, S. S., and S. Hazary. Variations of the lumbrical muscles of the hand. *Anat. Rec.* 136:501–504, 1960.

[8]Berolo, S., R. P. Wells, and B. C. Amick. Musculoskeletal symptoms among mobile hand-held device users and their relationship to device use: a preliminary study in a Canadian university population. *Appl. Ergon.* 42:371–378, 2011.

[9]Brand, P. W., K. C. Cranor, and J. C. Ellis. Tendon and pulleys at the metacarpophalangeal joint of a finger. *J. Bone Jt. Surg.* 57:779–784, 1975.

[10]Brand, P. W., and A. Hollister. Clinical mechanics of the hand. St. Louis: Mosby, 1993.

[11]Buford, Jr, W. L., S. Koh, C. R. Andersen, and S. F. Viegas. Analysis of intrinsic-extrinsic muscle function through interactive 3-dimensional kinematic simulation and cadaver studies. *J. Hand Surg. (A)* 30:1267–1275, 2005.

[12]Caetano, M Bf, W. M. Albertoni, and E. B. Caetano. Anatomical studies of the distal insertion of extensor pollicis longus. *Acta Ortopeica Brasileira* 12:118–124, 2004.

[13]Chadwick, E. K., D. Blana, A. J. van den Bogert, and R. F. Kirsch. A real-time, 3-D musculoskeletal model for dynamic simulation of arm movements. *IEEE Trans. Biomed. Eng.* 56(4):941–948, 2009.

[14]Chao, E. Y., K. N. An, W. Cooney, and R. Linscheid. Normative model of human hand, Biomechanics of the Hand. Singapore: World Scientific, pp. 5–30, 1989.

[15]Delp, S. L., F. C. Anderson, A. S. Arnold, P. Loan, A. Habib, and C. T. John. Opensim: open-source software to create and analyze dynamic simulations of movement. *IEEE Trans. Biomed. Eng.* 54(11):1940–1950, 2007.

[16]Delp, S. L., and J. P. Loan. A graphics-based software system to develop and analyze models of musculoskeletal structures. *Comput. Biol. Med.* 25(1):21–34, 1995.

[17]Ettema, G. J. C., G. Styes, and V. Kippers. The moment arms of 23 muscles segments of the upper limb with varying elbow and forearm positions: implications for motor control. *Hum. Mov. Sci.* 17:201–220, 1998.

[18]Fowler, N. K., A. C. Nicol, B. Condon, and D. Hadley. Method of determination of three dimensional index finger moment arms and tendon lines of action using high resolution MRI scans. *J. Biomech.* 34:791–797, 2001.

[19]Franko, O. I., T. M. Winters, T. F. Tirrell, E. R. Hentzen, and R. L. Lieber. Moment arms of the human digital flexors. *J. Biomech.* 44:1987–1990, 2011.

[20]Fregly, B. J., M. L. Boninger, and D. J. Reinkensmeyer. Personalized neuromusculoskeletal modeling to improve treatment of mobility impairments: a perspective from European research sites. *J. NeuroEng. Rehabil.* 9:18, 2012.

[21]Garner, B. A., and M. G. Pandy. The obstacle-set method for representing muscle paths in musculoskeletal models. *Comput. Methods Biomech. Biomed. Eng.* 3:1–30, 2000.

[22]Gatti, C. J., and R. E. Hughes. Optimization of muscle wrapping objects using simulated annealing. *Ann. Biomed. Eng.* 37:1342–1347, 2009.

[23]Gerbeaux, M., E. Turpin, and G. Lensel-Corbeil. Musculoarticular modeling of the triceps brachii. *J. Biomech.* 29(2):171–180, 1996.
[24]Greiner, T.M., 1991. Hand Anthropometry of US Army Personnel. United States Natick Research, Development and Engineering Center, Natick, MA, Document AD-A244 533.
[25]Hibbeler, R. C. Mechanics of Materials. Boston: Prentice Hall, 2013.
[26]Higginson, J. S., R. R. Neptune, and F. C. Anderson. Simulated parallel annealing within a neighborhood for optimization of biomechanical systems. *J. Biomech.* 38:1938–1942, 2005.
[27]Higginson, J. S., F. E. Zajac, R. R. Neptune, S. A. Kautz, and S. L. Delp. Muscle contributions to support during gait in an individual with post-stroke hemiparesis. *J. Biomech.* 39(10):1769–1777, 2006.
[28]Hogan, N. Mechanical impedance of single- and multi-articularsystems. In: Multiple Muscle Systems, edited by J. Winters, and S. Woo. NewYork: Springer, 1990, pp. 149–164.
[29]Holzbaur, K. R. S., W. M. Murray, and S. L. Delp. A model of the upper extremity for simulating musculoskeletal surgery and analyzing neuromuscular control. *Ann. Biomed. Eng.* 33(6):829–840, 2005.
[30]Kamper, D. G., H. C. Fischer, and E. G. Cruz. Impact of finger posture on mapping from muscle activation to joint torque. *Clin. Biomech.* 21:361–369, 2006.
[31]Kelley, C. T. Iterative Methods for Optimization. Philadelphia: SIAM, 1999.
[32]Ketchum, L. D., P. W. Brand, D. Thompson, and G. S. Pocock. The determination of moments for extension of the wrist generated by muscles of the forearm. *J. Hand Surg. (A)* 3:205–210, 1978.
[33]Kirkpatrick, S., C. D. Gelatt, and M. P. Vecchi. Optimization by simulated annealing. *Science* 220(4598):671–680, 1983.
[34]Kociolek, A. M., and P. J. Keir. Modelling tendon excursions and moment arms of the finger flexors: anatomic fidelity versus function. *J. Biomech.* 44:1967–1973, 2011.
[35]Kurse, M. U., H. Lipson, and F. J. Valero-Cuevas. Extrapolatable analytical functions for tendon excursions and moment arms from sparse datasets. *IEEE Trans. Biomed. Eng.* 59(6):1572–1582, 2012.
[36]Landsmeer, J. M. Studies in the anatomy of articulation. I. The equilibrium of the ''intercalated'' bone. *Acta Morphologica Neerlanddo – Scandinavica* 3:287–303, 1961.
[37]Lee, S. W., and D. G. Kamper. Modeling of multiarticular muscles: importance of inclusion of tendon-pulley interactions in the finger. *IEEE Trans. Biomed. Eng.* 56(9):2253–2262, 2009.
[38]Li, Z., C. C. Chang, P. G. Dempsey, L. Ouyang, and J. Duan. Validation of a three-dimensional hand scanning and dimension extraction method with dimension data. *Ergonomics* 51(11):1672–1692, 2008.
[39]Lloyd, D. G., and T. F. Besier. An EMG-driven musculoskeletal model to estimate muscle forces and knee joint moments *in vivo*. *J. Biomech.* 36:765–776, 2003.
[40]Lopes, M. M., W. Lawson, T. Scott, and P. J. Keir. Tendon and nerve excursion in the carpal tunnel in healthy and CTD wrists. *Clin. Biomech.* 26:930–936, 2011.
[41]Mahfouz, M. R., W. A. Hoff, R. D. Komistek, and D. A. Dennis. A robust method for registration of three-dimensional knee implant models to two-dimensional fluoroscopy images. *IEEE Trans. Med. Imaging* 22(12):1561–1574, 2003.
[42]Martin, J. R., M. L. Latash, and V. M. Zatsiorsky. Effects of the index finger position and force production on the flexor digitorum superficialis moment arms at the metacarpophalangeal joints- an magnetic resonance imaging study. *Clin. Biomech.* 27(5):453–459, 2012.
[43]Matsopoulos, G. K., K. K. Delibasis, N. A. Mouravliansky, P. A. Asvestas, K. S. Nikita, V. E. Kouloulias, and N. K. Uzunoglu. CT-MRI automatic surface-based registration schemes combining global and local optimization techniques. *Technol. Health Care* 11(4):219–232, 2003.
[44]McKay, J. L., and L. H. Ting. Optimization of muscle activity for task-level goals predicts complex changes in limb forces across biomechanical contexts. *PLoS Comput. Biol.* 8(4):e1002465, 2012.
[45]Murray, W. M., T. S. Buchanan, and S. L. Delp. Scaling of peak moment arms of elbow muscles with dimensions of the upper extremity. *J. Biomech.* 35:19–26, 2002.
[46]Murray, W. M., S. L. Delp, and T. S. Buchanan. Variation of muscle moment arms with elbow and forearm position. *J. Biomech.* 28(5):513–525, 1995.
[47]Neptune, R. R. Optimization algorithm performance in determining optimal controls in human movement analyses. *J. Biomech. Eng.* 121:249–252, 1999.
[48]Neptune, R. R., S. A. Kautz, and F. E. Zajac. Muscle contributions to specific biomechanical functions do not change in forward versus backward pedaling. *J. Biomech.* 33:155–164, 2000.
[49]Neptune, R. R., S. A. Kautz, and F. E. Zajac. Contributions of the individual ankle plantar flexors to support, forward progression and swing initiation during walking. *J. Biomech.* 34:1387–1398, 2001.
[50]Oh, S., M. Belohlaverk, C. Zhao, N. Osamura, M. E. Zobitz, K. N. An, and P. C. Amadio. Detection of differential gliding characteristics of the flexor digitorum superficialis tendon and subsynovial connective tissue using color Doppler sonographic imaging. *J. Ultrasound Med. Off. J. Am. Inst. Ultrasound Med.* 26(2):149–155, 2007.
[51]Pigeon, P., L. Yahia, and A. Feldman. Moment arms and lengths of human upper limb muscles as functions of joint angles. *J. Biomech.* 29(10):1365–1370, 1996.
[52]Qin, J., D. Lee, Z. Li, H. Chen, and J. T. Dennerlein. Estimating *in vivo* passive forces of the index finger muscles: exploring model parameters. *J. Biomech.* 43:1358–1363, 2010.
[53]Qin, J., M. Trudeau, J. Katz, B. Buchholz, and J. T. Dennerlein. Biomechanical loading on the upper extremity increases from single key to directional tapping. *J. Electromyogr. Kinesiol.* 21:587–594, 2011.
[54]Radwin, R.G., and S.A. Lavender, 1999. Work factors, personal factors, and internal loads: Biomechanics of work stressors. Work-related Musculoskeletal Disorders: Report, workshop summary, and workshop papers, pp. 116–151.
[55]Rankin, J. W., and R. R. Neptune. Musculotendon lengths and moment arms for a three-dimensional upper-extremity model. *J. Biomech.* 45:1739–1744, 2012.
[56]Rekimoto, J., 2002. Smartskin: An infrastructure for freehand manipulation on interactive surfaces. Proceedings of the SIGCHI conference on human factors in computing systems.
[57]Roloff, I., V. R. Schoffl, L. Vigouroux, and F. Quaine. Biomechanical model for the determination of the forces acting on the finger pulley system. *J. Biomech.* 39:915–923, 2006.

[58]Rubine, D. Specifying gestures by example. In: Proceedings of the 18th Annual Conference on Computer Graphics and Interactive Techniques. New York, NY: ACM, 1991, pp. 329–337. doi:10.1145/122718.122753.
[59]Sancho-Bru, J. L., A. Perez-Gonzalez, M. Vergara-Monedero, and D. Giurintano. A 3-D dynamic model of human finger for studying free movements. *J. Biomech.* 34:1491–1500, 2001.
[60]Sarojak, M., W. Hoff, R. Komistek, and D. Dennis. An interactive system for kinematic analysis of artificial joint implants. *Biomed. Sci. Instrum.* 35:9–14, 1999.
[61]Seth, A., M. Sherman, J. A. Reinbolt, and S. L. Delp. OpenSim: a musculoskeletal modeling and simulation framework for in silico investigations and exchange. *Symp. Hum. Body Dyn.* 2011:212–232, 2011.
[62]Soechting, J. F., and M. Flanders. Flexibility and repeatability of finger movements during typing: analysis of multiple degree of freedom. *J. Comput. Neurosci.* 4:29–46, 1997.
[63]Valero-Cuevas, F. J., M. E. Johanson, and J. D. Towles. Towards a realistic biomechanical model of the thumb: the choice of kinematic description may be more critical than the solution method or the variability/uncertainty of musculoskeletal parameters. *J. Biomech.* 36:1019–1030, 2003.
[64]van Soest, A. J., and L. J. R. R. Casius. The merits of a parallel genetic algorithm in solving hard optimization problems. *J. Biomech. Eng.* 125:141–146, 2003.
[65]Wang, K., E. P. McGlinn, and K. C. Chung. A biomechanical and evolutionary perspective on the function of the lumbrical muscle. *J. Hand Surg.* 39(1):149–155, 2014.
[66]Wu, J., K. N. An, R. G. Cutlip, and R. G. Dong. A practical biomechanical model of the index finger simulating the kinematics of the muscle/tendon excursions. *BioMed. Mater. Eng.* 20:89–97, 2010.
[67]Wu, M., and R. Balakrishna, 2003. Multi-finger and whole hand gestural interaction techniques for multi-user tabletop displays. Proceedings of the 16th annual ACM symposium on User interface software and technology.
[68]Yoshii, Y., H. R. Villarraga, J. Henderson, C. Zhao, K. N. An, and P. C. Amadio. Speckle tracking ultrasound for assessment of the relative motion of flexor tendon and subsynovial connective tissue in the human carpal tunnel. *Ultrasound Med. Biol.* 35(12):1973–1981, 2009.
[69]Zajac, F. E., and G. L. Cottlieb. Muscle and tendon: properties, models, scaling, and application to biomechancis and motor control. *Crit. Rev. Biomed. Eng.* 17(4):359–411, 1989.
[70]Zatsiorsky, V. M. Kinematics of human motion. Champaign, IL: Human Kinetics, 1998.
[71]Zhang, X., A. Kuo, and D. Chaffin. Optimization-based differential kinematic modeling exhibits a velocity-control strategy for dynamic posture determination in seated reaching movements. *J. Biomech.* 31:1035–1042, 1998.